Peculiarities in formation of smoke aerosol dispersion structure at thermal decomposition of coniferous wood.
2. Variations of temperature

R.F. Rakhimov, E.V. Makienko, and V.S. Kozlov

Institute of Atmospheric Optics,
Siberian Branch of the Russian Academy of Sciences, Tomsk

Received December 5, 2007

A series of smoke generation experiments in the Big Aerosol Chamber was carried out. Changes in particle size distribution and complex parameter of refraction (CPR) were studied under the growth of temperature of thermal decomposition of wood samples. The pyrolysis wood decomposition under temperature growth (from 350 up to 700°C) leads to a decrease of relative share of middle-size ($0.3 < r < 0.8$ microns) and large particles with $r > 1$ micron. As the temperature increases from 590 to 700°C, the relative share of absorbing formations grows. The real part of the CPR varies from 1.59 to 1.7, while the imaginary part changes from 0.005 to 0.020. At the final stages of pyrolysis size spectra become closer, and their volumetric distribution degenerates in the unimodal form of logarithmically normal distribution with the effective size $r_{\text{ef}} \approx r_m \approx 0.3$ microns and the width of dispersion parameter $2\ln^2\sigma \approx 1/12$. At a relatively low temperature ($T \sim 300$°C), the incomplete decomposition of coniferous wood is observed. This smoke exceeds high-temperature smokes in integral volume and particles sizes.

Introduction

Intensive development of modern technologies dealing with objects of nanometer range is connected with enhanced potential risks from fatal consequences for biological objects (BO) of uncontrolled waste products of different processes, for example, the increased concentration of nanoparticles (NP). Dispersed aerosols of nanometer size have a unique ability of penetration into BO and overpass the barriers in the path of intensive penetration of viruses and other microorganisms to the under-cell level of BO, including human organisms. In this connection, optical investigations of the processes determining formation, evolution, and sink of the finely dispersed component (FDC) of atmospheric aerosols are urgent also for such field of research as nanotoxicology, which deals with aerosol structures with sizes less than 100 nm.

It is revealed that the penetration of NP to the under-cell level of BO favors additional oxidation processes. In this context, a high concentration of NP in air can be considered as an aggressive medium for BO and people. Free penetration of NP significant concentrations into respiratory tract and other organs of a human being can lead to fatal consequences of mass destruction of cell structures, their anomalous functioning, mutation, and death.[1]

The process of thermal decomposition of materials is the simplest process providing for effective formation of such aerosols. The microstructure and optical properties of smokes for long time are the subject of instrumental researches.[2–4]

Earlier,[3] some peculiarities in formation of the finely dispersed aerosol in the process of low-temperature pyrolysis of wooden materials at variations of the initial mass of samples were considered based on smoke experiments in the Big Aerosol Chamber (BAC). The obtained results allowed studying in detail some peculiarities of formation of the smoke aerosol size spectrum at their passing from local volume of the thermal decomposition chamber (TDC) of the muffle oven (~ 4–5 liters) to the BAC of a volume of 1800 m.[3]

When analyzing the data of some experiments, it was mentioned that the level of accumulation and an effective sink of finely dispersed smokes depend on duration of stay of the aerosol-gas mixture (AGM) of particles and aerosol-producing compounds (APC) in TDC, as well as on disperse composition, which is forming during the mixture passing to BAC.

The increase of the relative content of particles of intermediate and coarse fractions with increasing mass of burnt samples increases the “coagulation” losses of fine particles ($r < 0.2$ μm). Active formation of intermediate fraction favors more effective cleaning of the air medium from finely dispersed particles, including the nanodispersion range. Their relative content in the size spectrum of smoke particles shows the tendency to a noticeable decrease during the process of smoke evolution in the chamber.

Technique for investigations

The spectral nephelometric measurements of the polarized components of the directed light-scattering coefficient for wooden smokes $\beta_s^{\lambda_i \theta_k}(t)$, km$^{-1}\cdot$sr^{-1} were used as initial data for optical diagnostics of temporal evolution of the smoke microstructure. Measurements were carried out with the use of the

0235-6880/08/04 252-05 $02.00

polarization nephelometer at five scattering angles θ_k: 15, 45, 110, 135, 165° and nine wavelengths λ in the range ~ 0.44–0.69 μm. Thus, 90 values of successively measured polarized components of the directed scattering coefficient were used for solving the inverse problem of light scattering and determination of microstructure variations of smoke parameters.

Since the process of measurement of so large set of parameters was carried out automatically at different time (complete cycle of measurements at all angles and wavelengths took 8–9 minutes), the obtained time dependences were synchronized by means of a special procedure. The regime of recording the light scattering parameters was controlled by a computer on the base of the developed algorithm with file-by-file accumulation of optical data. General problems of organization and statement of laboratory experiments with smokes in the BAC, the technique for calibration of the spectral nephelometer, the synchronization and smoothing of the measured data are considered in detail in Refs. 2 and 4.

Results of measurements and their analysis

The obtained results are shown in Fig. 1. It is seen that the measured light scattering signals have noticeable differences in the time dynamics at variations both in angles and wavelengths, especially at the stage of initial formation and development of the pyrolysis smokes.

After 10–12 hours of the development of the pyrolysis smokes, the disperse mixture passes to the stage of relaxation under the influence of effective sink of particles on the chamber walls. At this stage, all signals stably (almost exponentially) decrease, that corresponds to the natural tendency of the decrease of the total particle concentration. However, at the same time, the presented data show small deviations from the tendency of strictly exponential decrease, that evidences the long-term remaining weak inhomogeneities in the spatial distribution of smoke particles inside the BAC.

The presence of the aforementioned irregularities (uncoordinated at different wavelengths and scattering angles) is the obstacle for their direct use as initial data for solving the inverse problem. The thing is that the deviations due to irregularities and different times of recording the data noticeably increase the error in the conducted averaging, and, hence, in the initial data for solving the inverse problem. It is seen, first of all, in distortion of the retrieved distributions in the size range $r > 1.5$ μm, the optical contribution of which to the considered set of measured parameters is relatively small.

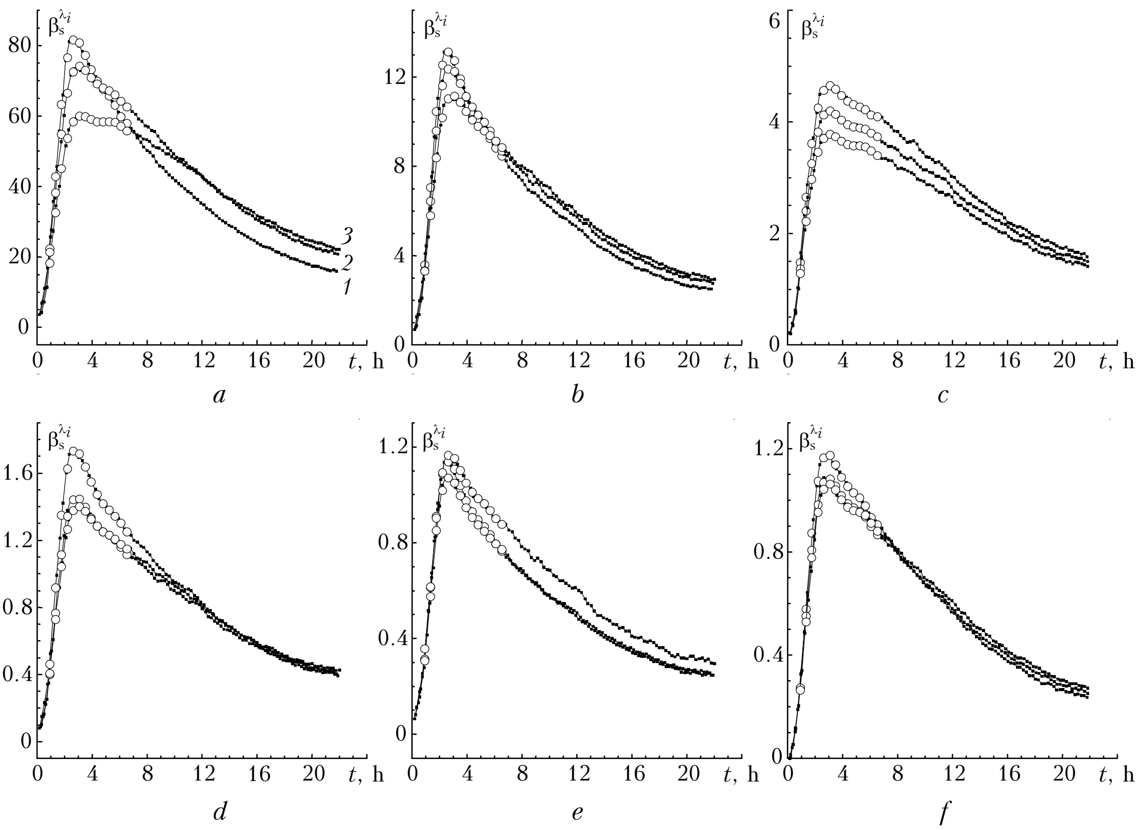

Fig. 1. Variations of the measured values of $\beta_s^{\lambda_i}(t)$, $km^{-1} \cdot sr^{-1}$ at three wavelengths λ: 0.44 (*1*); 0.56 (*2*); 0.69 μm (*3*) and decomposition temperature ($T \approx 540°C$) for perpendicularly polarized component at scattering angles θ_k: 15° (*a*); 45° (*b*); 165° (*c*); 110° (*d*); 135° (e) and parallelly polarized component at θ_k = 135° (*f*).

Application of a special synchronization procedure helps to average more correctly the results of spectral nephelometric measurements and to obtain the data on the size spectrum of smoke particles up to the radius of 2–2.5 μm due to decreasing the error in the initial data.

Figure 2 shows the results of inverting the spectral nephelometric measurements at two stages of the smoke development in experiments, in which the effect of the temperature between 515 and 700°C is studied.

Figure 2*a* illustrates the effect of the pyrolysis temperature on the particle volume distribution over radii at the stage of the maximal filling of BAC, i.e., at the stage when the signals measured with the spectral nephelometer have reached their maximum.

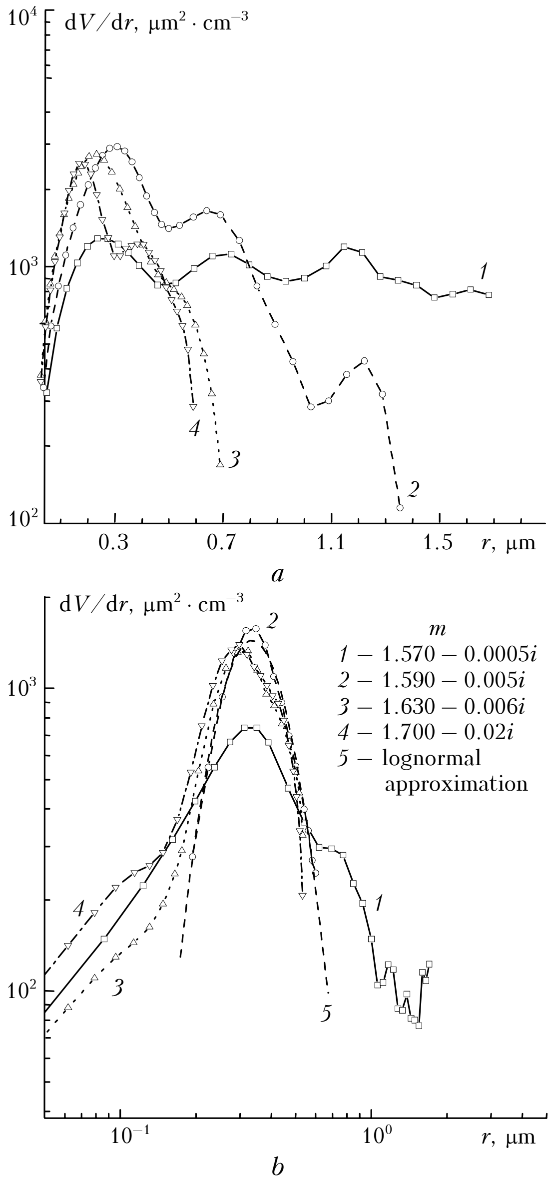

Fig. 2. Size distribution density of the total volume of particles in pyrolysis smokes at decomposition of 375 g of coniferous wood samples at different stages of the process: in 2 hours 40 min (maximum filling of BAC) (*a*); in 12 hours at initial $T = 515°$ (*1*); 590° (*2*); 640° (*3*); 700°C (*4*) (*b*).

As the temperature increases, finely dispersed particles become prevalent in the smoke microstructure due to the decrease of the large particle concentration. Optical characteristics of smokes at a temperature of 640°C and higher are completely determined by particles, the sizes of which (volume) are in the range $r < 0.6$ μm. The optical constants of the particulate matter also change. Estimates of the particles' complex refractive index, obtained from solution of the inverse problem ($m \approx 1.57 - 0.0005i$) at a temperature of 515°C (Fig. 2*b*) are typical for pyrolysis smokes. As the temperature increases, the real and imaginary parts of the complex refractive index increase (up to 1.7 and 0.02, respectively, at a temperature of 700°C), that evidences the increase of the relative fraction of absorbing compounds in the composition of smokes, first of all, the soot.

Note that the estimates of the complex refractive index in the experiments under discussion change only as a function of the temperature and remain invariable within the limits of the error in calculation at different stages of the process of thermal decomposition. For most experimental data in the regime of low-temperature ($T < 500$°C) pyrolysis of pine samples, the estimates of the complex refractive index fall in the range $n = 1.52$–1.58 (real part) at its imaginary part less than 0.001. However, overestimated values were obtained in some realizations: $n = 1.65$–1.68. The reason of these deviations is not clear and, evidently, is connected with neglecting of some factor in initial statement of the experiment.

At final stages of the pyrolysis smoke evolution the spectra noticeably approach to each other and then degenerate to the unimodal spectrum close to the lognormal distribution $2\ln^2\sigma \approx 1/12$ and the effective size $r_{\rm ef} \approx r_m \approx 0.3$ μm practically coincides with the mode r_m of the lognormal distribution:

$$\frac{\mathrm{d}V}{\mathrm{d}r} = \frac{V_0}{\sqrt{2\pi}\ln^2\sigma}\exp\left\{-\frac{\ln^2(r/r_m)}{2\ln^2\sigma}\right\}.$$

Figure 3 illustrates the transformation of the smoke microstructure as a function of the pyrolysis temperature in numerical estimates of the number concentration N, total cross section S, total volume V of particles, effective radius $r_{\rm ef}$, and their temporal dynamics.

It is seen that the rate of variation of the microstructure integral parameters depends on the reached level of the smoke particle concentration. The higher is this level, the faster are quantitative and qualitative variations of the size spectrum of smoke particles.

As the temperature in TDC increases, the effective radius of smoke particles stably decreases (Fig. 3*d*), and the decrease is particularly sharp up to $T \sim 640$°C. The temporal dependence $r_{\rm ef}(t)$ is transformed. The value of $r_{\rm ef}$ at a temperature of about 515°C monotonically decreases from 0.44 μm at the initial stages to 0.34 μm at the final stages of the process of the smoke evolution in the BAC. The rate of removing particles with $r > 1$ μm from the size spectrum mainly affects the shape of the temporal dependence $r_{\text{ef}}(t)$ in this case. As the smoke aerosol concentration increases simultaneously with the increase of the decomposition temperature (Fig. 3*c*) due to the increase of the number of fine particles, the intensity of their interaction between each other increases.

The effective size of smoke particles at a temperature of 590°C has the time dependence close to neutral, the shape of which is determined by the ratio of the rates of variation of the concentrations of particles of the first and the second submicrometer modes with gradual accumulation of the residual fraction of smoke aerosol (in volume) in size range 0.2–0.6 μm. At further temperature increase up to 640–700°C, large particles are absent in the particle size spectrum already at initial stages. The value of $r_{\text{ef}}(t)$ monotonically increases from 0.19 to 0.26 μm, which reflects the process of the growth of finely dispersed particles at their passing to the residual fraction of smoke.

Main peculiarities of the smoke microstructure in the regime of low-temperature pyrolysis are shown in Figs. 4 and 5 for the initial mass of pine samples M = 250 g.

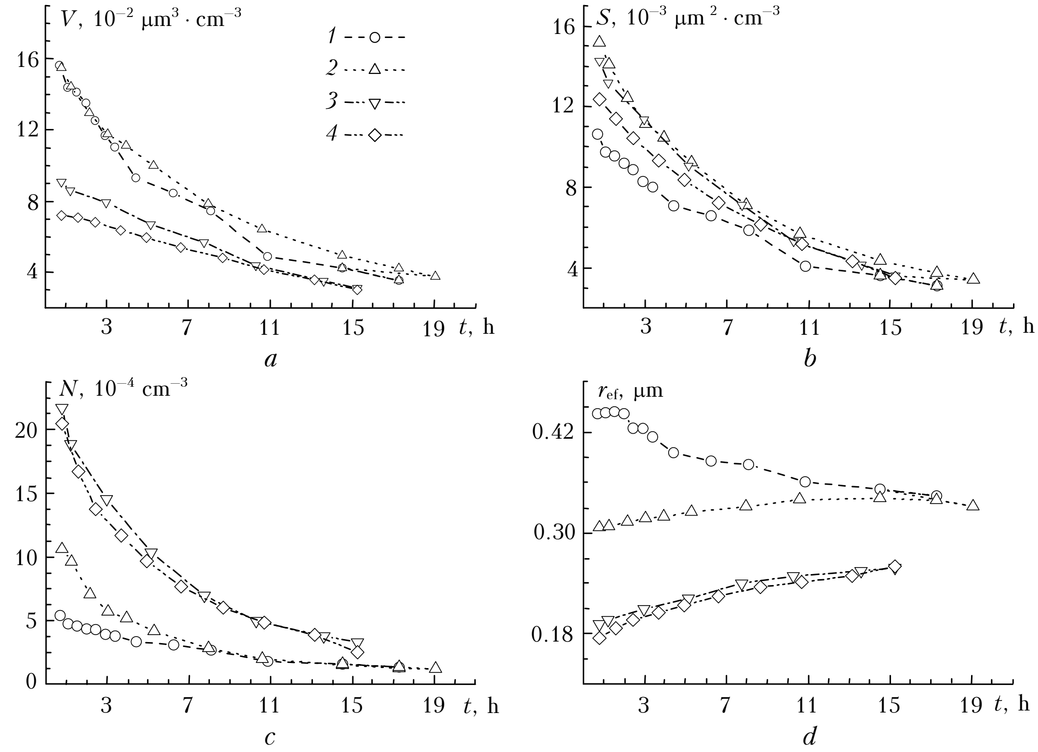

Fig. 3. Comparative time dynamics of variations of the integral parameters of the smoke microstructure as a function of the initial temperature of pyrolysis T ~ 515° (*1*); ~ 590° (*2*); ~ 640° (*3*); ~ 700°C (*4*).

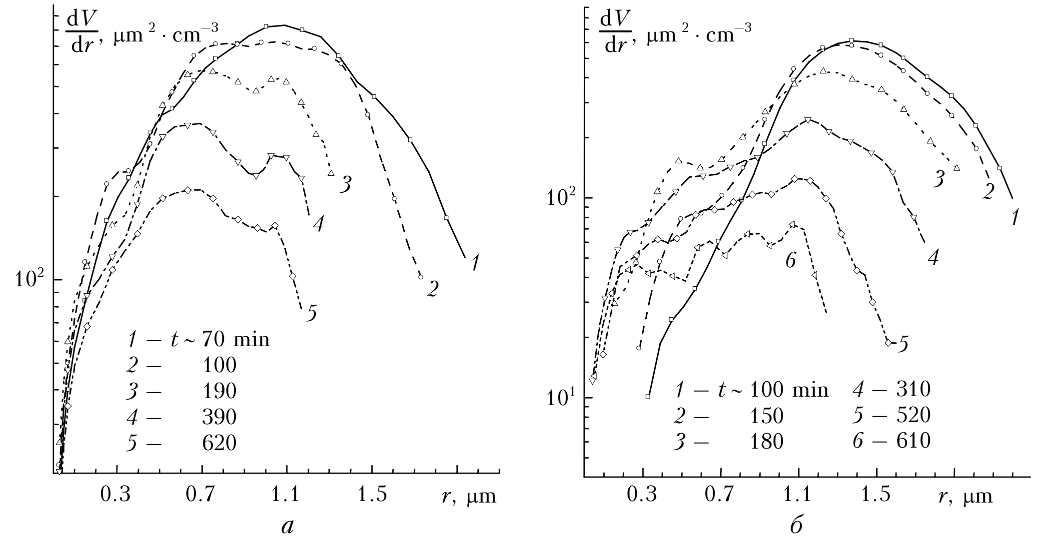

Fig. 4. Temporal variability of the particle volume size distribution density in smokes of low-temperature pyrolysis of coniferous wood samples: T = 430° (*a*); 356°C (*b*).

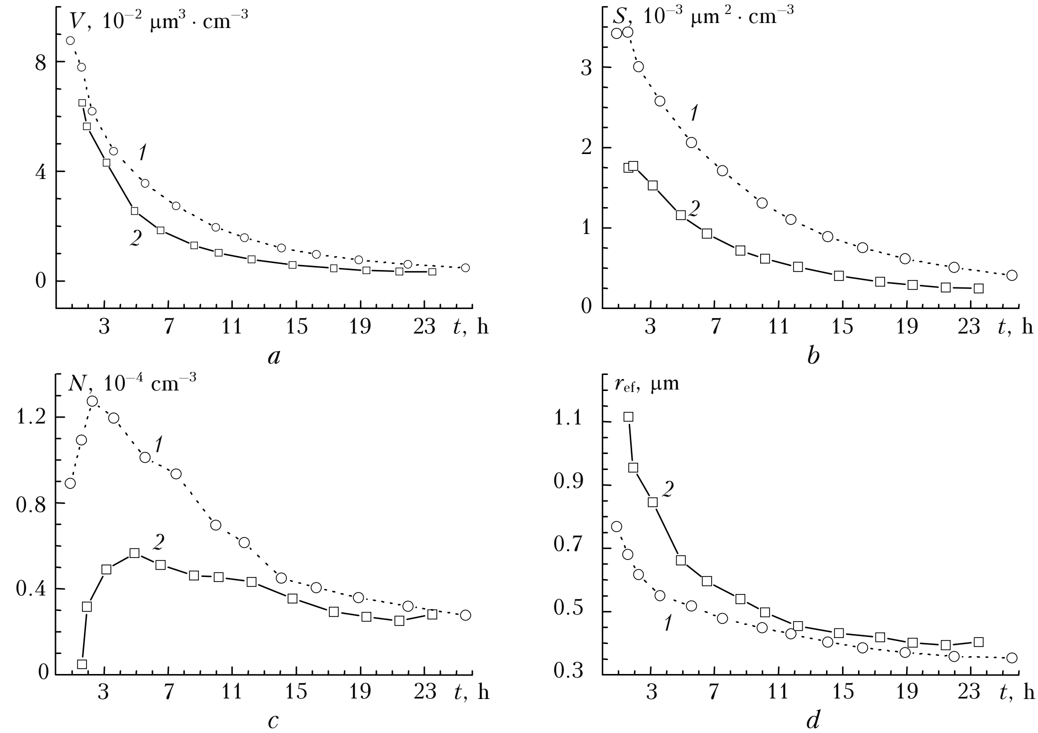

Fig. 5. Temporal dynamics of variations of the integral parameters of the microstructure of smoke of low-temperature pyrolysis: T = 430° (*1*); 356°C (*2*).

The tendency of increase (with decreasing temperature) of the mean size of particles generated in TDC is better pronounced in the time dynamics of $v(r)$ distributions (Fig. 4). The effective radius of particles, reaching the values $r_{ef} = 0.44$ μm in realizations shown in Fig. 3*d* (T = 515°C) increases up to 0.75 μm at $T \sim 430$°C and up to 1.2 μm at $T \sim 356$°C (Fig. 5*d*). The smoke microstructure at a temperature of ~ 430°C (Fig. 4*a*) at the maximum level of the measured signals ($t \sim 2$ hours) is represented by one sufficiently wide fraction of particles with the mode $r_m \approx 1$ μm. Position of this mode is shifted to the right up to the values of $r_m \approx 1.3$ μm at $T \sim 356$°C (Fig. 4*b*). In this case the initial temperature is already insufficient for fast generation of fine particles ($r < 0.7$ μm) and they are accumulated in optically significant concentrations only at later stages of the process (3–4 hours). Their fraction in the total volume of particles is small even at the stage of maximal accumulation.

Transformation of the smoke microstructure of the low-temperature pyrolysis in numerical estimates of the number concentration, total cross section, total volume of particles, effective radius r_{ef}, and their temporal dynamics is shown in Fig. 5. It is seen that in such regime the values of N, S, and V at all stages of smoke evolution in the BAC increase with the increasing temperature.

Conclusions

The fraction of large particles gradually decreases in the microstructure of smokes at initial stages of the processes in the regime of pyrolysis of wooden samples (pine) as the temperature increases from 350 to 700°C. The effective radius of particles of the disperse mixture changes from $r_{ef} = 1.2$ μm at a temperature of 356°C to 0.75 μm at T = ~ 430°C and reaches 0.18 μm at ~ 700°C. The optical characteristics of smokes at a temperature of 640°C and higher are completely determined by particles, the size of which (volume) are in the range $r < 0.6$ μm.

The smoke particles, generated in the process of pyrolysis at small temperatures of decomposition of coniferous wood samples, weakly absorb the visible radiation. The estimates of the complex refractive index for the main array of experimental data at temperatures < 500°C, obtained from solution of the inverse problem lie in the range of values n = 1.52–1.58 (real part) at the imaginary part less than 0.001 at all stages of the smoke evolution. As the temperature increases from 590 to 700°C, both the real part (from 1.59 to 1.7) and the imaginary part (from 0.005 to 0.02) increase, that evidences the increase of the relative fraction of absorbing compounds in the composition of smokes, first of all, the soot.

References

1. A.D. Maynard and R.J. Aitken, Nanotoxicology **1**, No. 3, 26–41 (2007).

2. R.F. Rakhimov, E.V. Makienko, V.S. Kozlov, M.V. Panchenko, and V.P. Shmargunov, Atmos. Oceanic Opt. **20**, No. 7, 561–567 (2007).

3. E.V. Makienko, D.M. Kabanov, R.F. Rakhimov, and S.M. Sakerin, Atmos. Oceanic Opt. **20**, No. 4, 287–293 (2007).

4. R.F. Rakhimov, Atmos. Oceanic Opt. **2**, No. 3, 206–212 (1989).